ARTICLE

doi:10.1038/nature16964

The peptidergic control circuit for sighing

Peng Li[1]*, Wiktor A. Janczewski[2]*, Kevin Yackle[1]*, Kaiwen Kam[2]†, Silvia Pagliardini[2]†, Mark A. Krasnow[1]§ & Jack L. Feldman[2]§

Sighs are long, deep breaths expressing sadness, relief or exhaustion. Sighs also occur spontaneously every few minutes to reinflate alveoli, and sighing increases under hypoxia, stress, and certain psychiatric conditions. Here we use molecular, genetic, and pharmacologic approaches to identify a peptidergic sigh control circuit in murine brain. Small neural subpopulations in a key breathing control centre, the retrotrapezoid nucleus/parafacial respiratory group (RTN/pFRG), express bombesin-like neuropeptide genes neuromedin B (*Nmb*) or gastrin-releasing peptide (*Grp*). These project to the preBötzinger Complex (preBötC), the respiratory rhythm generator, which expresses NMB and GRP receptors in overlapping subsets of ~200 neurons. Introducing either neuropeptide into preBötC or onto preBötC slices, induced sighing or *in vitro* sigh activity, whereas elimination or inhibition of either receptor reduced basal sighing, and inhibition of both abolished it. Ablating receptor-expressing neurons eliminated basal and hypoxia-induced sighing, but left breathing otherwise intact initially. We propose that these overlapping peptidergic pathways comprise the core of a sigh control circuit that integrates physiological and perhaps emotional input to transform normal breaths into sighs.

A sigh is a long, deep breath often associated with sadness, yearning, exhaustion or relief. Sighs also occur spontaneously, from several per hour in humans to dozens per hour in rodents[1,2]. Their recurrence during normal breathing enhances gas exchange and may preserve lung integrity by reinflating collapsed alveoli[2–4]. Sighing increases in response to emotional and physiological stresses, including hypoxia and hypercapnia, and in anxiety disorders and other psychiatric conditions where it can become debilitating[5,6].

The core of the breathing rhythm generator is the preBötC, a cluster of several thousand neurons in ventrolateral medulla. preBötC is required for inspiration and generates respiratory rhythms in explanted brain slices[7–10]. Each rhythmic burst activates premotoneurons and motoneurons that contract the diaphragm and other inspiratory muscles, generating a normal ('eupneic') breath[10]. Occasionally, a second preBötC burst immediately follows the first, and this 'double burst' leads to the augmented inspiration of a sigh[11–13], typically about twice the volume of a normal breath[14]. Thus, the command for normal breaths and sighs both appear to emanate from preBötC.

A variety of neuromodulators and neuropeptides[15,16], including frog bombesin[15], can influence sighing in rodents. However, the endogenous sigh control pathways have not been identified. We tested the effect of injecting bombesin into preBötC[17], and we screened for genes selectively expressed in breathing control centres (K.Y. and M.A.K., in preparation). These parallel approaches led to identification of two bombesin-like neuropeptide pathways connecting the RTN/pFRG, another medullary breathing control centre[18,19], to preBötC. We provide genetic, pharmacologic and neural ablation evidence that these pathways are critical endogenous regulators of sighing, and define the core of a dedicated sigh control circuit.

Neuromedin B links two breathing control centres

To identify breathing control genes, we screened >19,000 gene expression patterns in embryonic day 14.5 mouse hindbrain[20] (K.Y. and M.A.K., in preparation). The most specific pattern was *Nmb*, one of two genes encoding bombesin-like neuropeptides in mammals. *Nmb* is expressed in the medulla surrounding the lateral half of the facial nucleus, in or near RTN/pFRG in mouse (Fig. 1a, b and Extended Data Fig. 1a) and rat (Extended Data Fig. 1b). *Nmb* mRNA was also detected in the olfactory bulb and hippocampus (Extended Data Fig. 1c, d).

Nmb expression was further characterized using an *Nmb*-GFP BAC transgene with the *Nmb* promotor driving GFP expression, which reproduced the endogenous *Nmb* pattern (Fig. 1b, c). *Nmb*-GFP expressed in 206 ± 21 (mean ± standard deviation (s.d.), $n = 4$) RTN/pFRG neurons per side, most of which (92%, $n = 53$ cells scored) co-expressed *Nmb* mRNA (Extended Data Fig. 1e–h). In CLARITY-processed[21] brainstems, GFP-labelled cells surrounded the lateral half of the facial nucleus, with the highest density ventral and dorsal (Fig. 1d, e and Supplementary Video 1). This ventral parafacial region is the RTN, an important sensory integration centre for breathing[18,22,23]. Nearly all *Nmb*-GFP-positive cells (96%; $n = 202$ cells from 2 animals) co-expressed canonical RTN marker PHOX2B[24] (Fig. 1f), comprising one-quarter of the ~800 PHOX2B-positive RTN neurons[25].

Nmb-expressing neurons projected to preBötC (Fig. 1g, j). Punctate NMB staining was detected along the projections (Extended Data Fig. 2), with some puncta abutting somatostatin (SST)-positive preBötC neurons (Fig. 1h and Extended Data Fig. 2). Approximately 90 preBötC neurons expressed *Nmbr*, the G-protein-coupled receptor specific for NMB (Fig. 1i, see later). Thus, *Nmb*-expressing RTN/pFRG neurons may directly modulate preBötC neurons.

NMB injection into preBötC induces sighing

To investigate the function of this NMB pathway, the peptide was microinjected into preBötC of urethane-anaesthetized adult rats. Before injection, and after control (saline) injections (data not shown), airflow and diaphragmatic activity (DIA_{EMG}) showed the normal (eupneic) breathing pattern, with diaphragm activity bursts during inspiration (Fig. 2a, b and Extended Data Fig. 3a). Every minute or two, we observed a sigh ($44 \pm 10\,h^{-1}$, $n = 24$; unaffected by saline injection, Extended Data Fig. 3b), a biphasic double-sized breath coincident with a biphasic DIA_{EMG} event (Fig. 2b and Extended Data Fig. 3a, c–f). Amplitude

[1]Department of Biochemistry and Howard Hughes Medical Institute, Stanford University School of Medicine, Stanford, California 94305, USA. [2]Systems Neurobiology Laboratory, Department of Neurobiology, David Geffen School of Medicine, University of California Los Angeles, Los Angeles, California 90095, USA. †Present addresses: Department of Cell Biology and Anatomy, Chicago Medical School, Rosalind Franklin University of Medicine and Science, North Chicago, Illinois 60064, USA (K.K.); Department of Physiology, University of Alberta, Edmonton, Alberta T6G 2E1, Canada (S.P.).

*These authors contributed equally to this work.

§These authors jointly supervised this project.

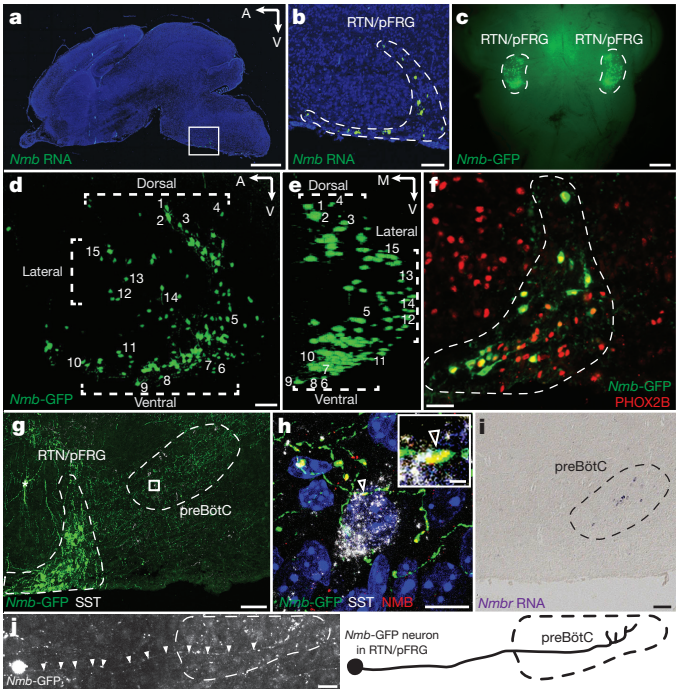

Figure 1 | NMB neuropeptide pathway neurons in breathing centre. **a**, P0 mouse brain section probed for *Nmb* mRNA (green) with DAPI counterstain (nuclei, blue). Scale bar, 1 mm. **b**, Boxed region (**a**) showing specific expression in RTN/pFRG. Scale bar, 100 μm. **c**, Whole mount P0 brainstem (ventral view) showing *Nmb*-GFP transgene expression (GFP, green) bilaterally in RTN/pFRG. Scale bar, 0.5 mm. **d**, **e**, Three-dimensional reconstruction (sagittal (**d**), coronal (**e**) projections) of CLARITY-cleared P14 *Nmb*-GFP brainstem. Note, RTN/pFRG expression ventral, dorsal, and lateral to facial nucleus. Numbers, representative neurons. A, anterior; V, ventral; M, medial. Scale bar, 100 μm. **f**, P0 *Nmb*-GFP-expressing neurons (green) in RTN/pFRG (dashed) co-express RTN marker PHOX2B (red). Scale bar, 50 μm. **g**, P7 *Nmb*-GFP-expressing neurons (green) project to preBötC (dashed). SST (somatostatin), preBötC marker (white). Asterisk indicates isolated GFP-labelled neuron in facial nucleus. Scale bar, 100 μm. **h**, Boxed region (**g**) with NMB co-stain (*z*-stack projection; optical sections, Extended Data Fig. 2). Arrowhead, NMB puncta (red) in *Nmb*-GFP-expressing projection (green) abutting preBötC neuron (SST, white). Scale bars, 10 μm (1 μm, inset). **i**, P7 ventral medulla section probed for *Nmbr* mRNA (purple) showing preBötC expression. Scale bar, 100 μm. **j**, Tiled image (left) and tracing (right) of *Nmb*-GFP neuron as in **g** projecting to preBötC. Scale bar, 30 μm.

and timescale of the first component of a sigh was indistinguishable from eupneic breaths, like human sighs[26]. Following bilateral NMB microinjection (100 nl, 3 μM) into preBötC, sighing increased 6–17-fold ($n = 5$; Fig. 2a, c, d and Extended Data Fig. 4a–e). The effect peaked several minutes after injection and persisted for 10–15 min afterwards.

We also tested NMB on explanted preBötC brain slices of neonatal mice, where inspiratory activity is detected as rhythmic bursts of preBötC neurons and hypoglossal (cranial nerve XII) motoneuron output (Fig. 2e). Occasionally, a burst with two peaks ('doublet') was observed (Fig. 2e)[11], a proposed *in vitro* signature of a sigh (see Methods). Addition of 10 nM and 30 nM NMB increased doublet frequency by 1.7-fold ($P = 0.005$; $n = 7$) and twofold, respectively ($P = 0.003$; $n = 7$) (Fig. 2e, f). The overall frequency of bursts and doublets together was unchanged ($P = 0.2$; $n = 7$), implying NMB converts inspiratory bursts into sighs; indeed, in some preparations every inspiratory burst was converted to a doublet (Extended Data Fig. 5). We conclude that NMB acts directly on preBötC to increase sighing.

NMBR signalling maintains basal sighing

To determine if NMB signalling is required for sighing, we monitored breathing of awake, unrestrained *Nmbr*$^{-/-}$ knockout mice. Wild-type controls (C57BL/6) sighed $40 \pm 11\ h^{-1}$, whereas *Nmbr*$^{-/-}$ mutants sighed $29 \pm 10\ h^{-1}$ ($n = 4$; $P < 0.001$) (Fig. 2g). Sighing was also transiently reduced ~50% in anaesthetized rats by NMBR inhibition following bilateral preBötC injection of the antagonist BIM23042 (100 nl, 6 μM) (Fig. 2h and Extended Data Fig. 6a–d and 7a). The antagonist effect was selective for sighing as it did not significantly alter respiratory rate (117 ± 14 vs 109 ± 6 breaths per minute with antagonist, $n = 4$, $P = 0.14$) or tidal volume (2.1 ± 0.1 vs 2.0 ± 0.3 ml, $n = 4$, $P = 0.46$), and similar selectivity was observed for the *Nmbr* mutant (respiratory rate 218 ± 22 vs 254 ± 22 in *Nmbr*$^{-/-}$ mice, $n = 4$, $P = 0.06$; tidal volume 0.30 ± 0.03 vs 0.31 ± 0.04 ml, $n = 4$, $P = 0.88$). Thus NMBR signalling in preBötC maintains basal sighing.

A related neuropeptide pathway modulates sighing

Nmbr mutations and inhibition reduced but did not abolish sighing, suggesting involvement of other pathways. *Grp*, the only other bombesin-like neuropeptide gene in mammals[27], was expressed in several dozen cells in the dorsal RTN/pFRG in mouse (Fig. 3a) and rat (Extended Data Fig. 8e), plus scattered cells in nucleus tractus solitarius (NTS) and parabrachial nucleus (PBN), two other breathing circuit nuclei[10,28] (Extended Data Fig. 8a–d). GRP-positive projections were traced from RTN/pFRG to preBötC, with some GRP puncta abutting SST-positive preBötC neurons (Extended Data Fig. 8f–i). GRP signals through GRPR, the receptor most similar to NMBR. *Grpr* mRNA was detected in ~160 mouse preBötC neurons (Fig. 3b and see later), suggesting GRP can also directly modulate preBötC function.

To determine if GRP regulates sighing, the neuropeptide (100 nl, 3 μM) was injected bilaterally into preBötC of anaesthetized rats. Sighing increased 8–16-fold ($n = 5$; Fig. 3c and Extended Data Fig. 4f–j). GRP (3 nM) application to mouse preBötC brain slices also increased sighing, producing 1.7-fold more doublets ($P = 0.003$; $n = 9$; Fig. 3d). Thus, GRP can induce sighing through direct modulation of preBötC neurons, like NMB.

To determine if GRPR signalling is required for sighing, we monitored breathing in *Grpr*$^{-/-}$ knockout mice. Their basal sigh rate (22 ± 9 per hour, $n = 4$) was half that of control wild-type mice (Fig. 3e), whereas eupneic breathing appeared normal (respiratory rate 218 ± 22 vs 210 ± 16 in *Grpr*$^{-/-}$, $n = 4$, $P = 0.57$; tidal volume 0.30 ± 0.03 vs 0.28 ± 0.01 ml, $n = 4$, $P = 0.23$). GRPR inhibition by bilateral preBötC injection of antagonist RC3095 (100 nl, 6 μM) in anaesthetized rats also transiently decreased sighing by ~50% ($n = 4$), followed by rapid rebound and overshoot (Fig. 3f and Extended Data Fig. 6e–h). There was no significant change in other respiratory parameters (respiratory rate 117 ± 12 vs 111 ± 11 with antagonist, $n = 4$, $P = 0.34$; tidal volume 2.0 ± 0.2 vs 1.9 ± 0.1 ml, $n = 4$, $P = 0.11$). Thus, GRPR signalling in preBötC also maintains basal sighing.

Expression patterns, loss-of-function phenotypes and localized pharmacological manipulations of NMBR and GRPR signalling in preBötC suggest that NMB–NMBR and GRP–GRPR pathways can independently modulate sighing.

NMBR and GRPR are the critical pathways in sighing

To explore the relationship between NMB and GRP pathways, we compared expression patterns of the neuropeptides and receptors within mouse RTN/pFRG and preBötC. *Nmb* and *Grp* were detected in non-overlapping neuronal subpopulations, with *Nmb* neurons distributed throughout RTN/pFRG and *Grp* neurons restricted to the dorsal domain (Fig. 4a–d). In contrast, receptor expression patterns in preBötC overlapped (Fig. 4e–h), with 40 ± 16 neurons expressing *Nmbr*, 113 ± 45 expressing *Grpr*, and 49 ± 9 expressing both ($n = 3$).

To explore functional interactions, we injected both neuropeptides into preBötC of anaesthetized rats. Sigh rate increased 12–24-fold, which was similar or slightly beyond that of either neuropeptide alone (Fig. 4i and Extended Data Fig. 4k–o). When NMBR and GRPR pathways were simultaneously inhibited by bilateral injection of both antagonists, BIM23042 (100 nl, 6 μM) and RC3095 (100 nl, 6 μM), sighing was

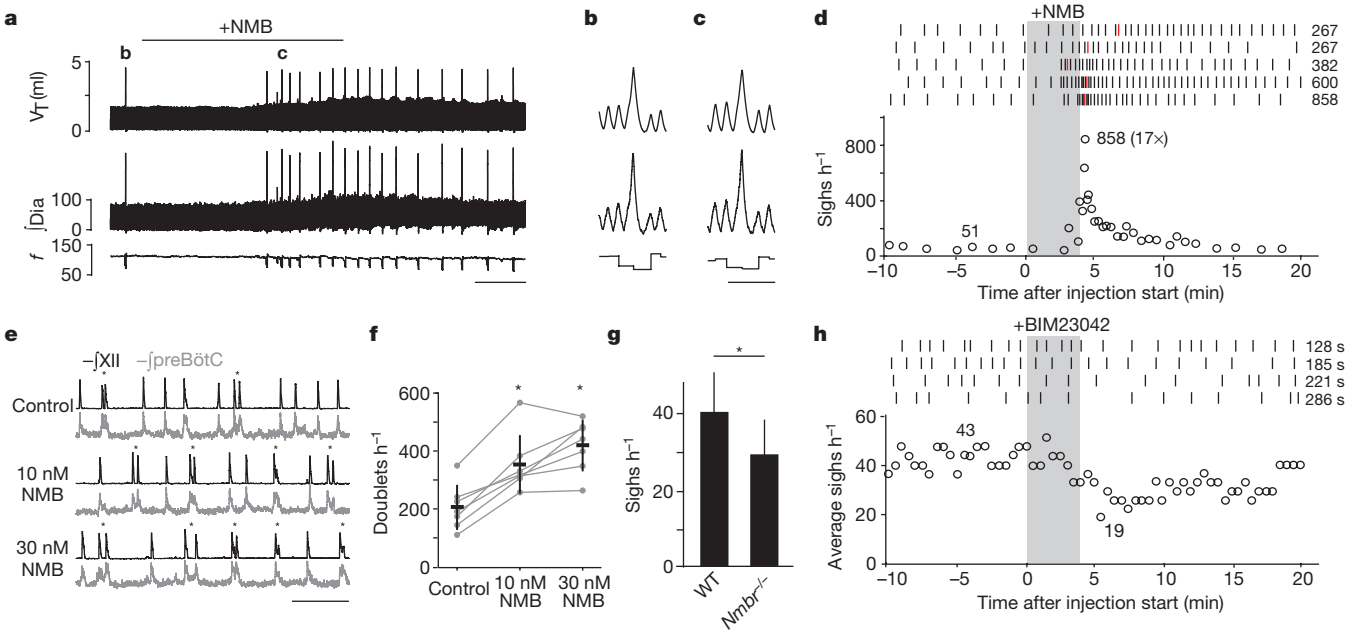

Figure 2 | NMB effect on breathing. a–c, Breathing activity of anaesthetized rat following bilateral NMB injection (100 nl, 3 μM) into preBötC. Note increased sighing (spikes in tidal volume (V_T), integrated diaphragm activity (∫Dia)), but little change in respiratory rate (frequency, *f*). Bar, 1 min. **b**, **c**, Similar, stereotyped waveforms of spontaneous (**b**) and NMB-induced (**c**) sighs (from **a**; also Extended Data Fig. 3a, c–f). Bar, 2 s. **d**, Quantification of (**a**). Top: raster plots of sighs (tics) in five rats following NMB injection (grey); numbers, highest instantaneous sigh rate (red tics). Bottom: instantaneous sigh rate of bottom raster plot; numbers, average instantaneous sigh rate before and maximum (and fold increase) after injection. **e**, Integrated hypoglossal nerve (∫XII; black) and preBötC neural activity (∫preBötC; grey) in preBötC slices containing indicated NMB concentrations. NMB increases doublets (*), a sigh signature in slices. Bar, 10 s. **f**, Quantification of (**e**) (data as mean ± s.d. $n = 7$; $^*P < 0.05$ by paired *t*-test). **g**, Basal sigh rate in C57BL/6 wild-type (WT) and $Nmbr^{-/-}$ mice. $n = 4$; data as mean ± s.d.; $^*P < 0.001$ by unpaired *t*-test. **h**, Effect on sighing in anaesthetized rats of bilateral preBötC injection (grey) of NMBR antagonist BIM23042 (100 nl, 6 μM). Top: raster plots; numbers, longest inter-sigh intervals (s, seconds) following injection. Bottom: sliding average sigh rate (bin 4 min; slide 30 s); numbers, average rate before (left) and minimum binned rate after injection (right).

severely reduced or eliminated ($n = 6$; Fig. 4j, Extended Data Fig. 6i–n). Thus, NMBR and GRPR pathways can independently modulate sighing, and together are required for basal sighing *in vivo*.

Effect of NMBR and GRPR neuron ablation

To determine if preBötC NMBR- and GRPR-expressing neurons function specifically in sigh control, we ablated them using bombesin (BBN), which binds both receptors[27], conjugated to saporin (BBN–SAP), a ribosomal toxin that induces neuronal death when internalized[8]. Three days after bilateral BBN–SAP injection (200 nl, 6.15 ng per side) into preBötC of rats, sighing was reduced ~80%, from 24 ± 3 h^{-1} before injection to 5 ± 4 h^{-1} three days after injection ($P = 5 \times 10^{-6}$; $n = 7$) (Fig. 5a). The effect was selective as other aspects of breathing and behaviour appeared normal. Five days after injection, sighing was almost completely (~95%) abolished, decreasing to 0.6 ± 0.6 h^{-1} ($P = 10^{-8}$; $n = 6$; Fig. 5a). Other aspects of breathing and

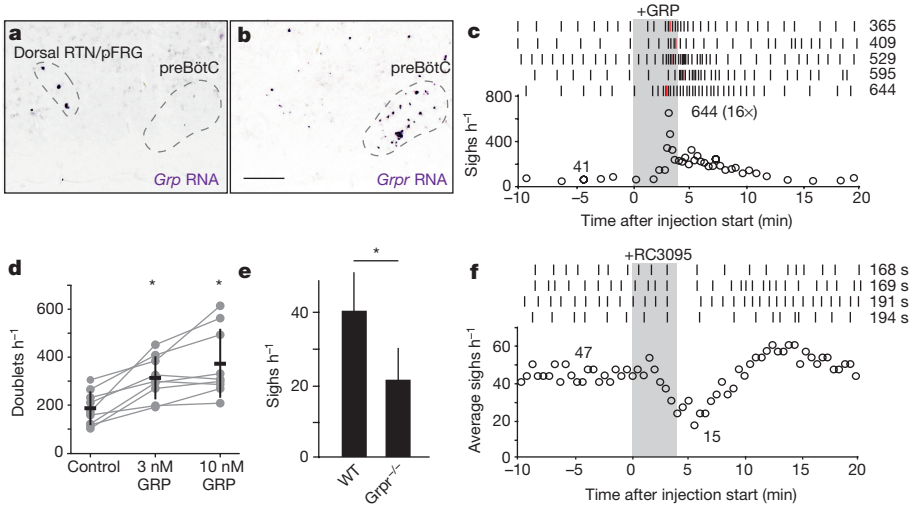

Figure 3 | GRP neuropeptide pathway expression and function in breathing. a, **b**, Sagittal ventral medulla sections of P7 mice probed for *Grp* (**a**) or *Grpr* (**b**) mRNA (purple). Scale bar, 200 μm. **c**, Effect on sighing of bilateral preBötC injection of GRP (100 nl, 3 μM), as in Fig. 2d. **d**, Effect of GRP on doublets (sighs) in preBötC slices, as in Fig. 2f. Data as mean ± s.d. $n = 9$; $^*P < 0.05$ by paired *t*-test. **e**, Basal sigh rate in C57BL/6 wild-type (WT) and $Grpr^{-/-}$ mice. $n = 4$; data as mean ± s.d.; $^*P < 0.001$ by Mann–Whitney *U*-test. **f**, Effect on sighing of bilateral preBötC injection of GRPR antagonist RC3095 (100 nl, 6 μM), as in Fig. 2h.

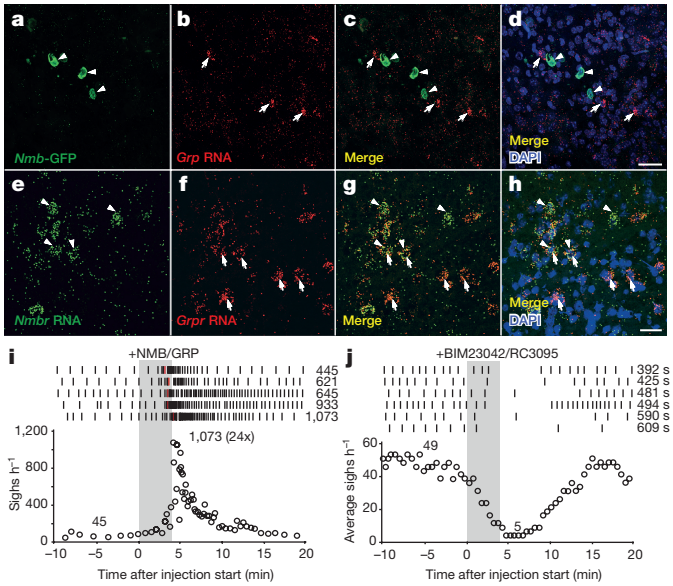

Figure 4 | Interactions between NMB and GRP pathways in sighing. **a**–**d**, RTN/pFRG section of P7 *Nmb*-GFP mouse immunostained for GFP (green, arrowheads) and probed for *Grp* mRNA (red, arrows). Note no expression overlap. Scale bar, 30 μm. **e**–**h**, preBötC section of P28 mouse probed for *Nmbr* mRNA (green, arrowheads) and *Grpr* mRNA (red, arrows). Note partial expression overlap. Scale bar, 30 μm. **i**, Effect on sighing of bilateral preBötC injection of both NMB (100 nl, 3 μM) and GRP (100 nl, 3 μM) as in Fig. 2d. **j**, Effect on sighing of bilateral preBötC injection (100 nl, 6 μM) of both NMBR and GRPR antagonists (BIM23042, RC3095) as in Fig. 2h.

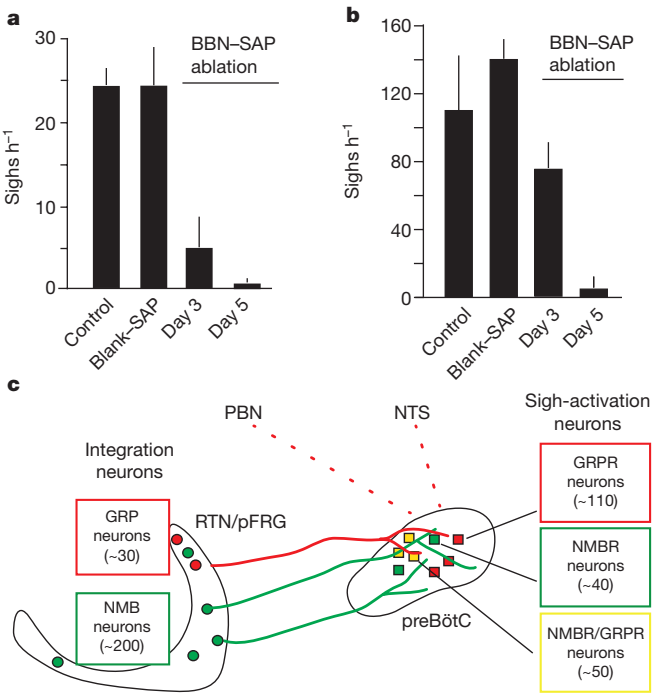

Figure 5 | Effect on sighing of ablating preBötC NMBR-expressing and GRPR-expressing neurons. **a**, **b**, Basal (**a**) and hypoxia-induced (**b**) sigh rates before (control) and 3 or 5 days after preBötC injections of bombesin–saporin (200 nl, 6.2 ng; BBN–SAP ablation) to ablate NMBR- and GRPR-expressing neurons, or 5 days after saporin alone (200 nl, 6.2 ng; Blank–SAP). Data as mean ± s.d.; $P < 0.05$ (BBN–SAP ablation vs control rats at day 3 or 5 for both room air (**a**) and hypoxia (**b**)). Sample size $n = 6$ (control), 3 (Blank–SAP), 7 (day 3), 6 (day 5). **c**, Model of peptidergic sigh control circuit. NMB- and GRP-expressing neurons in RTN/pFRG (and perhaps GRP-expressing neurons in NTS and PBN) receive physiological and perhaps emotional input from other brain regions, stimulating neuropeptide secretion. This activates receptor-expressing preBötC neurons expressing their receptors, which transform the normal preBötC rhythm to sighs. (Because neuropeptides induce sighs separated by normal breaths (Fig. 2a), there must be some refractory mechanism in or downstream of receptor-expressing neurons that temporarily prevents a second sigh.)

behaviour again appeared generally intact (Extended Data Fig. 9a, b). However, after 5 days we noted increasing episodes of apneas or disordered breathing, possibly a consequence of the loss of sighing (see Discussion). Ablation prevented sigh induction by exogenous BBN infusion into the cisterna magna, confirming preBötC *Nmbr*- and *Grpr*-expressing neurons were eliminated (Extended Data Fig. 9c). However, BBN infusion still triggered intense scratching and licking, demonstrating that the *Grpr* and *Nmbr* neurons outside the preBötC required for these behaviours[29] remained intact. We conclude that preBötC *Nmbr* and *Grpr*-expressing neurons have a critical and selective function in basal sighing.

NMBR and GRPR neurons are critical for induced sighs

To determine if the *Nmbr* and *Grpr*-expressing neurons are also important for physiologically-induced sighs, we examined BBN–SAP rats exposed to hypoxia (8% O_2). In control rats injected with unconjugated SAP, sighing increased from 24 ± 5 to 140 ± 14 h^{-1} under hypoxia ($n = 3$, $P = 0.01$). In contrast, five days after BBN–SAP injection, sigh rate under hypoxia was 5.1 ± 7.9 h^{-1} ($n = 6$, $P = 0.2$, hypoxia vs room air at day 5; Fig. 5b); three of these rats did not sigh in room air (21% O_2) and no sighs were triggered by hypoxia. In BBN–SAP rats, hypoxia increased respiratory rate from 150 ± 5 to 230 ± 19 breaths per min, demonstrating ventilatory response to hypoxia was intact. Thus, *Nmbr*-expressing and *Grpr*-expressing neurons are also critical for hypoxia-induced sighing, but not other respiratory responses to hypoxia.

Discussion

Our results show sighing is controlled by two largely parallel bombesin-like neuropeptide pathways, NMB and GRP, which mediate signalling between key medullary breathing control centres. Approximately 200 *Nmb*-expressing and ~30 *Grp*-expressing neurons in neighbouring domains of RTN/pFRG, a region implicated in integrating respiratory sensory cues and generation of active expiration[23,28,30], project to preBötC, the respiratory rhythm generator. A total of 7% (~200) of preBötC neurons express *Nmbr* (~40 neurons), *Grpr* (~110) or both receptors (~50), activation of which increased sighing 6-fold to 24-fold, whereas sighing was effectively abolished by inhibition or deletion of the receptors, or ablation of the receptor-expressing neurons.

We propose the above neurons, perhaps with *Grp*-expressing NTS and PBN neurons, comprise the core of a peptidergic sigh control circuit, with the neuropeptide-expressing neurons integrating inputs from sites monitoring physiological and perhaps emotional state (Fig. 5c). Excitation of these neurons and secretion of either neuropeptide activates the cognate receptor-expressing preBötC neurons, which initiate sighs by altering activity of other preBötC neurons to convert normal breaths to sighs. This might occur by a burst of NMB and/or GRP secretion triggering a second inspiratory signal in the preBötC during or immediately after the first, resulting in a single, double-sized breath. Alternatively, NMB and GRP secretion might be more gradually modulated, causing concentration-dependent bursts in activity of receptor-expressing neurons or a shift in preBötC properties towards states favouring more frequent doublet bursts.

A priority will be to elucidate the full circuit and properties of the constituent neurons, including its integration with other peptides and neurotransmitters that influence sighing[15,16] and with normal breathing and other behaviours. A curious aspect of the circuit already apparent is the central role of two partially overlapping and closely related neuropeptide pathways. Do NMB- and GRP-expressing neurons receive different inputs and have distinct sensing functions, and do the three

sets of receptor-expressing neurons (NMBR, GRPR, NMBR + GRPR) converge on the same preBötC neurons to effect a sigh, or signal to different preBötC neurons producing distinct types of sighs?

A striking aspect of our results is the selectivity of the circuit for sighing. Inhibition of the pathways, and even ablation of receptor-expressing neurons, had little effect on other aspects of breathing, at least in the short term. This can now be exploited to test the classical hypothesis for the physiological function of sighing—re-expansion of alveoli that collapse during breathing and maintenance of lung integrity[2–4], and to investigate psychological benefits. Identification of the key neuropeptide pathways suggests pharmacologic approaches for controlling excessive sighing and inducing sighs in patients that cannot breathe deeply on their own. Dozens of molecularly distinct preBötC neuronal types have been identified recently (K.Y. and M.A.K., in preparation); perhaps they serve similarly specific roles in other respiratory-related behaviours like yawning, sniffing, crying, and laughing.

Online Content Methods, along with any additional Extended Data display items and Source Data, are available in the online version of the paper; references unique to these sections appear only in the online paper.

Received 28 May; accepted 30 December 2015.
Published online 8 February 2016.

1. Haldane, J. S., Meakins, J. C. & Priestley, J. G. The effects of shallow breathing. *J. Physiol. (Lond.)* **52,** 433–453 (1919).
2. McCutcheon, F. H. Atmospheric respiration and the complex cycles in mammalian breathing mechanisms. *J. Cell. Physiol.* **41,** 291–303 (1953).
3. Knowlton, G. C. & Larrabee, M. G. A unitary analysis of pulmonary volume receptors. *Am. J. Physiol.* **147,** 100–114 (1946).
4. Reynolds, L. B. Characteristics of an inspiration-augmenting reflex in anesthetized cats. *J. Appl. Physiol.* **17,** 683–688 (1962).
5. Bartlett, D. Origin and regulation of spontaneous deep breaths. *Respir. Physiol.* **12,** 230–238 (1971).
6. Maytum, C. K. Sighing dyspnea: A clinical syndrome. *J. Allergy* **10,** 50–55 (1938).
7. Smith, J. C., Ellenberger, H. H., Ballanyi, K., Richter, D. W. & Feldman, J. L. Pre-Bötzinger complex: a brainstem region that may generate respiratory rhythm in mammals. *Science* **254,** 726–729 (1991).
8. Gray, P. A., Janczewski, W. A., Mellen, N., McCrimmon, D. R. & Feldman, J. L. Normal breathing requires preBötzinger complex neurokinin-1 receptor-expressing neurons. *Nature Neurosci.* **4,** 927–930 (2001).
9. Tan, W. *et al.* Silencing preBötzinger complex somatostatin-expressing neurons induces persistent apnea in awake rat. *Nature Neurosci.* **11,** 538–540 (2008).
10. Feldman, J. L., Del Negro, C. A. & Gray, P. A. Understanding the rhythm of breathing: so near, yet so far. *Annu. Rev. Physiol.* **75,** 423–452 (2013).
11. Kam, K., Worrell, J. W., Janczewski, W. A., Cui, Y. & Feldman, J. L. Distinct inspiratory rhythm and pattern generating mechanisms in the preBötzinger complex. *J. Neurosci.* **33,** 9235–9245 (2013).
12. Lieske, S. P., Thoby-Brisson, M., Telgkamp, P. & Ramirez, J. M. Reconfiguration of the neural network controlling multiple breathing patterns: eupnea, sighs and gasps. *Nature Neurosci.* **3,** 600–607 (2000).
13. Ruangkittisakul, A. *et al.* Generation of eupnea and sighs by a spatiochemically organized inspiratory network. *J. Neurosci.* **28,** 2447–2458 (2008).
14. Caughey, J. L. Jr. Analysis of breathing patterns. *Am. Rev. Tuberc.* **48,** 382 (1943).
15. Niewoehner, D. E., Levine, A. S. & Morley, J. E. Central effects of neuropeptides on ventilation in the rat. *Peptides* **4,** 277–281 (1983).
16. Ramirez, J. M. The integrative role of the sigh in psychology, physiology, pathology, and neurobiology. *Prog. Brain Res.* **209,** 91–129 (2014).
17. Janczewski, W. A., Pagliardini, S., Cui, Y. & Feldman, J. L. Sighing after vagotomy. *Proc. Society of Neuroscience Conference* (New Orleans, 2012).
18. Smith, J. C., Morrison, D. E., Ellenberger, H. H., Otto, M. R. & Feldman, J. L. Brainstem projections to the major respiratory neuron populations in the medulla of the cat. *J. Comp. Neurol.* **281,** 69–96 (1989).
19. Onimaru, H. & Homma, I. A novel functional neuron group for respiratory rhythm generation in the ventral medulla. *J. Neurosci.* **23,** 1478–1486 (2003).
20. Diez-Roux, G. *et al.* A high resolution atlas of the transcriptome in the mouse embryo. *PLoS Biol.* **9,** e1000582 (2011).
21. Tomer, R. *et al.* Advanced CLARITY for rapid and high-resolution imaging of intact tissues. *Nature Protocols* **9,** 1682–1697 (2014).
22. Mulkey, D. K. *et al.* Respiratory control by ventral surface chemoreceptor neurons in rats. *Nature Neurosci.* **7,** 1360–1369 (2004).
23. Stornetta, R. L. *et al.* Expression of Phox2b by brainstem neurons involved in chemosensory integration in the adult rat. *J. Neurosci.* **26,** 10305–10314 (2006).
24. Guyenet, P. G. & Bayliss, D. A. Neural control of breathing and CO_2 homeostasis. *Neuron* **87,** 946–961 (2015).
25. Lazarenko, R. M. *et al.* Acid sensitivity and ultrastructure of the retrotrapezoid nucleus in Phox2b–EGFP transgenic mice. *J. Comp. Neurol.* **517,** 69–86 (2009).
26. Bendixen, H. H., Smith, G. M. & Mead, J. Pattern of ventilation in young adults. *J. Appl. Phyiol.* **19,** 195–198 (1964).
27. Jensen, R. T. *et al.*, International Union of Pharmacology. LXVIII. Mammalian bombesin receptors: nomenclature, distribution, pharmacology, signaling, and functions in normal and disease states. *Pharmacol. Rev.* **60,** 1–42 (2008).
28. Guyenet, P. G., Stornetta, R. L. & Bayliss, D. A. Central respiratory chemoreception. *J. Comp. Neurol.* **518,** 3883–3906 (2010).
29. Lee, H., Naughton, N. N., Woods, J. H. & Ko, M. C. Characterization of scratching responses in rats following centrally administered morphine or bombesin. *Behav. Pharmacol.* **14,** 501–508 (2003).
30. Pagliardini, S. *et al.* Active expiration induced by excitation of ventral medulla in adult anesthetized rats. *J. Neurosci.* **31,** 2895–2905 (2011).

Supplementary Information is available in the online version of the paper.

Acknowledgements We thank M. Sunday for providing the *Nmbr*$^{-/-}$ and *Grpr*$^{-/-}$ mice, Y. Zhang for providing rat tissues, and K. Wada and E. Wada for plasmid constructs for *in situ* hybridization probes. We also thank members of the Krasnow and Feldman laboratories for comments. This work was supported by the Howard Hughes Medical Institute (M.A.K.), NIH grants HL70029, HL40959 and NS72211 (J.L.F.), a Walter V. and Idun Berry postdoctoral fellowship (P.L.), the NIH Medical Scientist Training Program (K.Y.), and CIHR and AIHS postdoctoral fellowships (S.P.). M.A.K. is an investigator of the Howard Hughes Medical Institute.

Author Contributions W.A.J. and S.P. performed experiments showing the effects on sighing of bombesin injection into the preBötC and ablation of receptor-expressing neurons with bombesin–saporin. K.Y. performed the screen that discovered *Nmb* expression in the respiratory centres. P.L. performed experiments identifying and characterizing expression of *Nmb*, *Grp* and their receptors. W.A.J., P.L., and K.Y. performed genetic and pharmacology experiments on *Nmb* and *Grp* pathways. K.K. performed *in vitro* slice experiments. W.A.J., K.K., P.L., S.P., and K.Y. analysed data. J.L.F., W.A.J., K.K., M.A.K., P.L., and K.Y. conceived experiments, interpreted data and wrote the manuscript.

Author Information Reprints and permissions information is available at www.nature.com/reprints. The authors declare no competing financial interests. Readers are welcome to comment on the online version of the paper. Correspondence and requests for materials should be addressed to M.A.K. (krasnow@stanford.edu) or J.L.F. (feldman@g.ucla.edu).

METHODS

Animals. All procedures were carried out in accordance with animal care standards in National Institutes of Health (NIH) guidelines, and approved by the University of California, Los Angeles Animal Research Committee, or Stanford Institutional Animal Care and Use Committee. All mouse strains used were in the C57BL/6 genetic background. *Nmb*-GFP BAC transgenic mice (Tg(Nmb-EGFP)IT50Gsat/Mmucd), carrying EGFP coding sequence inserted upstream of the Nmb start codon in the BAC, were from the Mutant Mouse Regional Resource Centers (catalogue number 030425-UCD, https://www.mmrrc.org). *Nmbr*$^{-/-}$ and *Grpr*$^{-/-}$ null mutant mice, in which exon 2 of the endogenous gene was replaced by a neomycin-resistance cassette using homologous recombination, have been described[31,32]. Male Sprague Dawley rats were from Charles River.

***In situ* hybridization, immunostaining and reporter expression.** For *in situ* hybridization, mouse brains were harvested and fixed overnight in 4% paraformaldehyde in phosphate buffered saline (PBS), cryopreserved in 30% sucrose and embedded in optical cutting temperature compound (OCT). Transverse sections were cut at 16–20 μm and stored at −80 °C until use. Sections were post-fixed in 4% paraformaldehyde before treatment with hydrochloric acid, proteinase K, and then triethanolamine/acetic anhydride. Hybridization was carried out with *in vitro* transcribed and digoxygenin-labelled riboprobes at 58 °C overnight. Signal was detected using alkaline phosphatase-coupled anti-digoxigenin (DIG) primary antibody (Roche) and nitro blue tetrazolium chloride and bromochloroindolyl phosphate (NBT/BCIP) Reagent Kit (Roche) or using Horse Radish Peroxidase-coupled anti-DIG primary antibody (Roche) and Tyramide Signal Amplification plus Fluorescent Substrate Kit (PerkinElmer).

For double fluorescent *in situ* hybridization, tissue was harvested, embedded in OCT and then sectioned. Sections were fixed in 4% paraformaldehyde, dehydrated and treated with pretreatment reagent (Advanced Cell Diagnostics). Double fluorescent *in situ* assay was then performed using proprietary RNAscope technology (Advanced Cell Diagnostics) with cyanine 3 labelled *Nmbr* probes and fluorescein isothiocyanate labelled *Grpr* probes.

For *Nmb*-GFP reporter expression analysis, the brains of *Nmb*-GFP mice were harvested and fixed overnight in 4% paraformaldehyde and then cryopreserved at 4 °C in 30% sucrose overnight. Tissue was embedded in OCT and sectioned at 10–40 μm. Tissue sections were rinsed with PBT (PBS + 0.1% Tween), blocked with 3% bovine serum (BSA) in PBT for 1 h, and incubated with primary antibody overnight at 4 °C. Sections were rinsed in PBT and incubated for 1 h at room temperature with species-specific secondary antibodies. Primary antibodies were: chicken anti-GFP (Abcam 13970; used at 1:1,000 dilution), goat anti-PHOX2B (Santa Cruz, sc-13224; 1:200 dilution), rabbit anti-NMB (Sigma-Aldrich, SAB1301059; 1:100 dilution), rabbit anti-GRP (Immunostar 20073; 1:4,000 dilution), and rat anti-SST (Millipore, MAB354; 1:50 dilution). Secondary antibodies included donkey anti-chicken (Jackson Immuno Research; 1:400 dilution), donkey anti-rat (Jackson Immuno Research; 1:400 dilution), donkey anti-rabbit (Jackson Immuno Research; 1:400 dilution) and donkey anti-goat (Invitrogen; 1:500 dilution).

For *Nmb*-GFP expression analysis in samples prepared by CLARITY[21], *Nmb*-GFP mice were perfused with PBS and formaldehyde-acrylamide hydrogel, and brain tissue was harvested and incubated in hydrogel monomer solution at 4 °C for 3 days. Tissue was then embedded in polymerized hydrogel by raising the temperature to 37 °C for 3 h. Blocks of 1 mm thickness were cut and washed in 4% sodium dodecyl sulphate (SDS) in sodium borate buffer at 37 °C for 2 to 3 weeks. Samples were washed with PBST for 2 days and incubated in FocusClear (CelExplorer), and GFP fluorescence was imaged on a Zeiss LSM780 confocal microscope.

Sigh monitoring and analysis. For awake animals, individual animals were placed in a whole body plethysmography chamber (Buxco) at room temperature (22 °C) in 21% O_2 (for normoxia) or 8% O_2 (for hypoxic challenge) balanced with N_2. Sighs were identified in plethysmography traces by the characteristic biphasic ramp, the augmented flow in the second phase of the inspiratory effort and the prolongation of expiratory time following the event. Sighs were also confirmed by visual monitoring of breathing behaviour. Given the high amplitude and distinctive waveform of sighs relative to standard eupneic breaths, sighs were unambiguously identified by both visual and computer-assisted scoring; no difference was detected in direct comparisons between methods or observers, so visual scoring was used. Female 8-week-old mice (*Nmbr*$^{-/-}$, *Grpr*$^{-/-}$, or C57BL/6 as wild-type control) were acclimated to the chamber for 10 min, and then the first fifteen recorded sighs were used to calculate the sigh rate. Similar sigh rates were observed for each animal when assayed on different days. Rats were acclimated to the chamber for ~1 h, and then baseline sigh rate and respiratory frequency were calculated for the next 2 h. For hypoxic (8% O_2) challenge, analysis was continued for 30 min under the hypoxic condition.

For anaesthetized rats, the trachea was cannulated and connected to a pneumotachograph (GM Instruments) to record airflow. A flow calibration was performed after every experiment along with a calculation of tidal volume (V_T) by digital integration. To monitor diaphragm activity, wire electrodes (Cooner Wire) were implanted into the diaphragm and electromyogram (EMG) signal sampled at 2 kHz (Powerlab 16SP; AD Instruments). Signal was rectified and digitally integrated (time constant of 0.1) to obtain a moving average using LabChart Pro 8 (AD Instruments) and Igor Pro 6 (Data Matrix) software. Sighs were identified in the airflow measurements as above and validated by double peaks in the EMG recordings.

preBötC injection of NMB and GRP agonists and antagonists. Male Sprague Dawley rats ($n = 24$) weighing 320–470 g were anaesthetized with urethane (1.5 g per kg), isoflurane (0.3–0.7 vol%), and ketamine (20 mg per kg per hour) and injected i.p. with atropine (0.3 mg per kg), then placed in a supine position in a stereotaxic instrument (David Kopf Instruments). A tracheostomy tube was placed in the trachea through the larynx, and the basal aspect of the occipital bone was removed to expose the ventral medulla. Injections were placed 750 μm caudal from the most rostral root of the hypoglossal nerve (RRXII), 2 mm lateral to the midline, and 700 μm dorsal to the ventral medullary surface. Small corrections were made to avoid puncturing blood vessels on the medulla. Microinjection was done using a series of pressure pulses (Picospritzer; Parker-Hannifin) applied to the open end of micropipettes, with air pressure set so that each pulse ejected ~5 nl and a total volume of 0.1 μl was injected on each side. The concentration of injected neuropeptides and antagonists were: NMB, 3 μM; GRP, 3 μM; NMB and GRP, 3 μM each; BIM23042 (ref. 33), 6 μM; RC3095 (ref. 34), 6 μM; BIM23042 and RC3095, 6 μM each. To verify the accuracy of the injections, fluorescent polystyrene beads (0.2 μm FluoSpheres (Invitrogen; catalogue #F8811, #F8763 or #F8807); 2–5% vol) were added to the injected solutions, and following injection and physiological measurements the location of the fluorescent beads was visualized in wet tissue double stained for reelin and choline acetyltransferase (ChAT) to identify the preBötC.

Ablation of NMBR and GRPR-expressing preBötC neurons. Bilateral preBötC injections of saporin conjugated with either bombesin (BBN–SAP; Advanced Targeting System; 200 nl, 6.2 ng) or a non-targeted peptide (blank SAP; Advanced Targeting System; 200 nl, 6.2 ng) were performed in 300–350 g rats under anaesthesia (ketamine (90 mg per kg), and xylazine (10 mg per kg), administered i.p) using standard aseptic procedures. Rats were positioned on a stereotaxic frame with bregma 5 mm below lambda. The occipital bone was exposed and a small window was opened to perform BBN–SAP injections with a 40 μm diameter tip glass pipette inserted into the preBötC. Coordinates were (in mm): 0.9 rostral, 2.0 lateral, and 2.8 ventral to the obex. The electrode was left in place for 5 min after injection to minimize backflow of solution up the electrode track. After injection, a fine polyethylene cannula was implanted and cemented to the occipital bone to deliver BBN into the fourth ventricle. Neck muscles and skin were sutured back at the end of the surgery and rats were allowed to recover with pain medication, food and water ad libitum. Blank–SAP and BBN–SAP treated rats were tested for hypoxia (8% O_2 balanced with nitrogen, 30 min challenge) five days after surgery. Blank–SAP and BBN–SAP treated rats were also tested for response to BBN infusion in the cistern magna six days after surgery. The cannula implanted in the fourth ventricle was connected to a fine polyethylene tubing under isoflurane anaesthesia, and after recovery and placement of rats in a plethysmographic chamber, 10 μg of BBN diluted in 20 μl sterile saline was delivered followed by a 20 μl saline washout. Sigh rate and respiratory rate were calculated for 30 min following infusion and compared to pre-infusion values.

***In vitro* slice preparation, recording, and analysis.** Rhythmic 550-μm-thick transverse medullary slices containing the preBötC and XII nerve from neonatal C57BL/6 mice (P0–5) were prepared as described previously[11]. The medullary slice was cut in artificial cerebrospinal fluid (ACSF) containing (in mM): 124 NaCl, 3 KCl, 1.5 $CaCl_2$, 1 $MgSO_4$, 25 $NaHCO_3$, 0.5 NaH_2PO_4, and 30 D-glucose, equilibrated with 95% O_2 and 5% CO_2 (4 °C, pH = 7.4). For recording, extracellular K^+ was raised to 9 mM to replace excitatory afferent drive lost in the cutting process. Slices were perfused at 27 °C and 4 ml min^{-1} and allowed to equilibrate for 30 min. Respiratory activity reflecting suprathreshold action potential (AP) firing from populations of neurons was recorded as XII bursts from either XII nerve roots and as population activity directly from the preBötC using suction electrodes and a MultiClamp 700A or 700B (Molecular Devices, Sunnyvale, CA, USA), filtered at 2–4 kHz and digitized at 10 kHz. Digitized data were analysed off-line using custom procedures written for IgorPro (Wavemetrics, Portland, OR, USA). Activity was full-wave rectified and digitally integrated with a Paynter filter with a time constant of 20 ms with either custom built electronics or using custom procedures in MATLAB (Mathworks, Natick, MA, USA).

Burst detection and analysis of respiratory-related activity recorded in full-wave rectified XII output or preBötC population recordings were performed using custom software written in IgorPro. Burst parameters were normalized to the mode of the data in the baseline condition. Although there are several proposed definitions of sighs in slice preparations[12,13], here we used 'doublets' (double-peaked bursts) as the *in vitro* signature of sighs because, in our preparations, doublets detected both in preBötC neural population activity measurements and cranial nerve XII output recordings shared the increased inspiratory and expiratory duration of sighs[11]. Furthermore, as demonstrated here, doublet rate increased following application of NMB or GRP to preBötC slice preparations (Figs 2 and 3 and Extended Data Fig. 5), as did sigh rate *in vivo* following preBötC injection of the same neuropeptides (Figs 2 and 3). The frequency and waveform of doublets in slice preparations does not closely match those of sighs in intact animals, presumably due to the absence *in vitro* of important inputs modulating burst shape; indeed, the doublets more closely resemble sighs in vagotomized animals, where they appear as equal amplitude double-peaked breaths[11,17]. We scored a burst as a doublet if the burst displayed a second peak that reached 20% or more of the amplitude of the first burst, and this second peak occurred after more than twice the time from start to peak or if the burst had a duration longer than eight times the time from start to peak. All doublets were verified by visual inspection to exclude multipeaked bursts and two bursts that were too far apart. Measured doublet intervals were converted to a calculated per hour doublet rate.

Statistics. Data are represented as mean ± standard deviation (s.d.). Statistical significance was uniformly set at a minimum of $P < 0.05$. For comparisons of two groups, the assumption for normal distribution was determined by the Shapiro–Wilk test with the critical W value set at 5% significance level. The t-tests were conducted, with the exception in Fig. 3e, in which a Mann–Whitney U-test was used. For statistical comparisons of more than two groups, an ANOVA was first performed. In most cases, a two-way repeated measures ANOVA was used for comparisons of various parameters in different conditions and for making comparisons across different events. If the null hypothesis (equal means) was rejected, post-hoc paired t-tests were then used for pairwise comparisons of interest. Individual P values are reported, but Holm–Bonferroni analysis for multiple comparisons was conducted to correct for interactions between the multiple groups. Histograms were normalized by the total sample size to generate plots of the relative frequency of each value where the y value of each bin represents the fraction of the total number of samples for that experiment. Randomization and blinding were not used. No statistical method was used to predetermine sample size.

31. Ohki-Hamazaki, H. *et al.* Functional properties of two bombesin-like peptide receptors revealed by the analysis of mice lacking neuromedin B receptor. *J. Neurosci.* **19,** 948–954 (1999).
32. Wada, E. *et al.* Generation and characterization of mice lacking gastrin-releasing peptide receptor. *Biochem. Biophys. Res. Commun.* **239,** 28–33 (1997).
33. Orbuch, M. *et al.* Discovery of a novel class of neuromedin B receptor antagonists, substituted somatostatin analogues. *Mol. Pharmacol.* **44,** 841–850 (1993).
34. Qin, Y. *et al.* Inhibitory effect of bombesin receptor antagonist RC-3095 on the growth of human pancreatic cancer cells in vivo and in vitro. *Cancer Res.* **54,** 1035–1041 (1994).

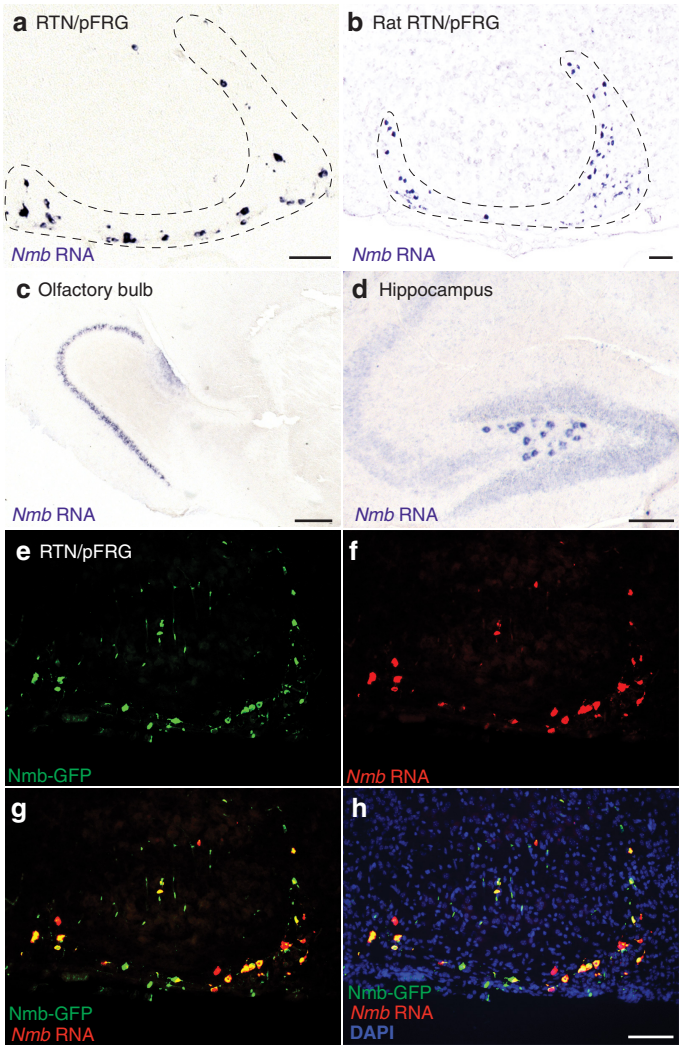

Extended Data Figure 1 | Expression of *Nmb* in rodent brain. **a, b**, Sagittal sections of P7 mouse (**a**) and P7 rat (**b**) brain showing RTN/pFRG region probed for *Nmb* mRNA expression (purple) by *in situ* hybridization as in Fig. 1. Scale bars, 100 μm. **c**, **d**, *Nmb* expression as in **a** showing regions outside ventrolateral medulla. *Nmb* is expressed in mouse olfactory bulb (**c**) and hippocampus (**d**). Scale bars, 200 μm (**c**) and 100 μm (**d**). **e–h**, Section through RTN/pFRG brain region of P0 transgenic *Nmb*-GFP mouse immunostained for GFP (green) and probed for *Nmb* mRNA (red) by *in situ* hybridization. Blue, DAPI nuclear stain. *Nmb*-GFP and *Nmb* mRNA are mainly co-expressed in the same cells. Scale bar, 100 μm.

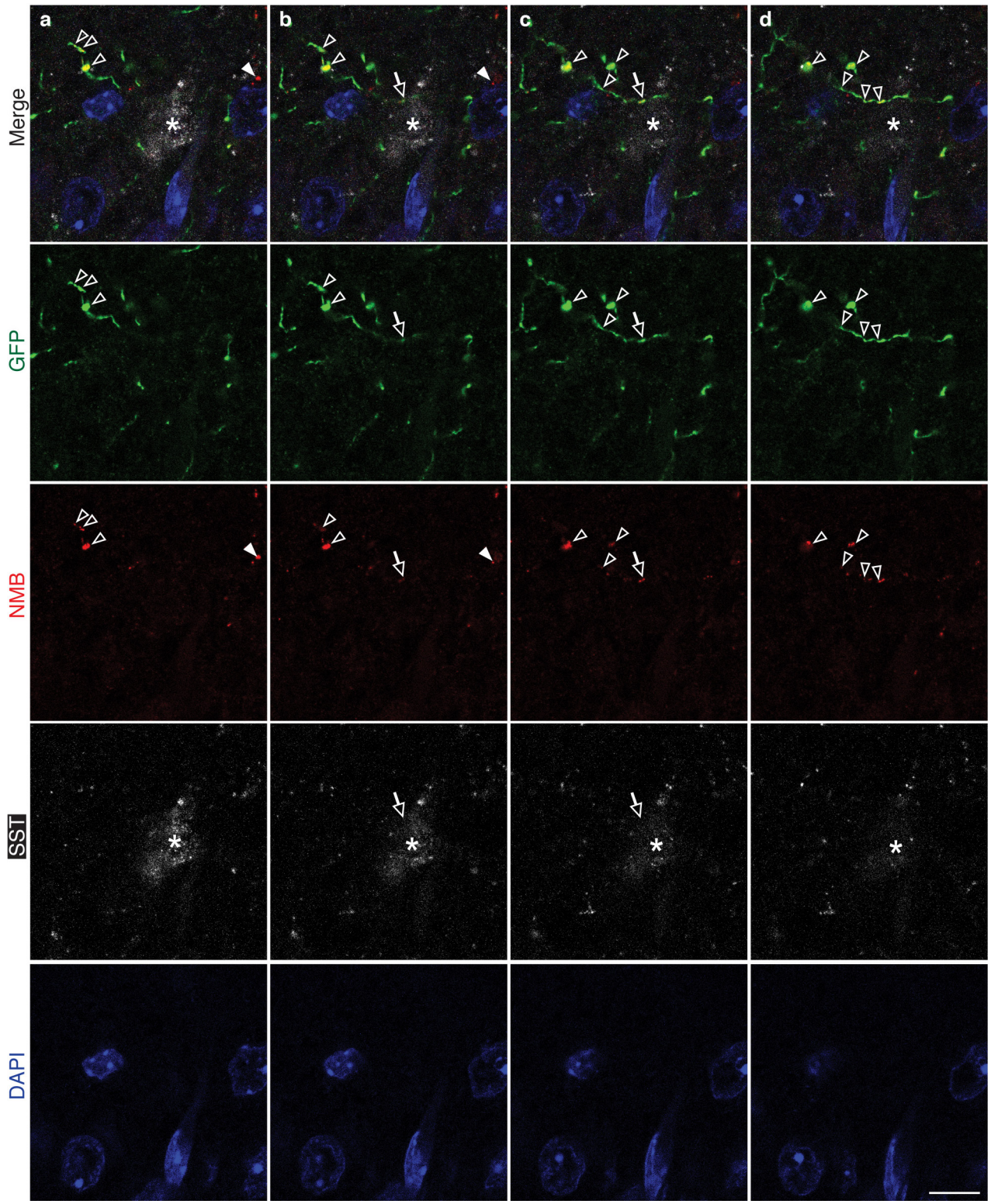

Extended Data Figure 2 | Serial confocal preBötC sections showing *Nmb*-GFP projections contain puncta of NMB. a–d, Serial confocal optical sections (0.6 μm apart) through preBötC brain region of *Nmb*-GFP mouse immunostained for GFP (green), NMB (red), preBötC marker SST (white), and DAPI (blue) as in Fig. 2h. Note the GFP-positive projection with a puncta of NMB (yellow, open arrows in **b**, **c**) directly abutting an SST positive neuron (asterisk). Most NMB puncta (open arrowheads) were detected within GFP-positive projections as expected, and only a small fraction of NMB puncta (closed arrowhead) were detected outside them; NMB outside *Nmb*-GFP projections could be secreted protein or the rare *Nmb*-expressing cells that do not co-express the *Nmb-GFP* transgene (see Extended Data Fig. 1e–h). Scale bar, 20 μm.

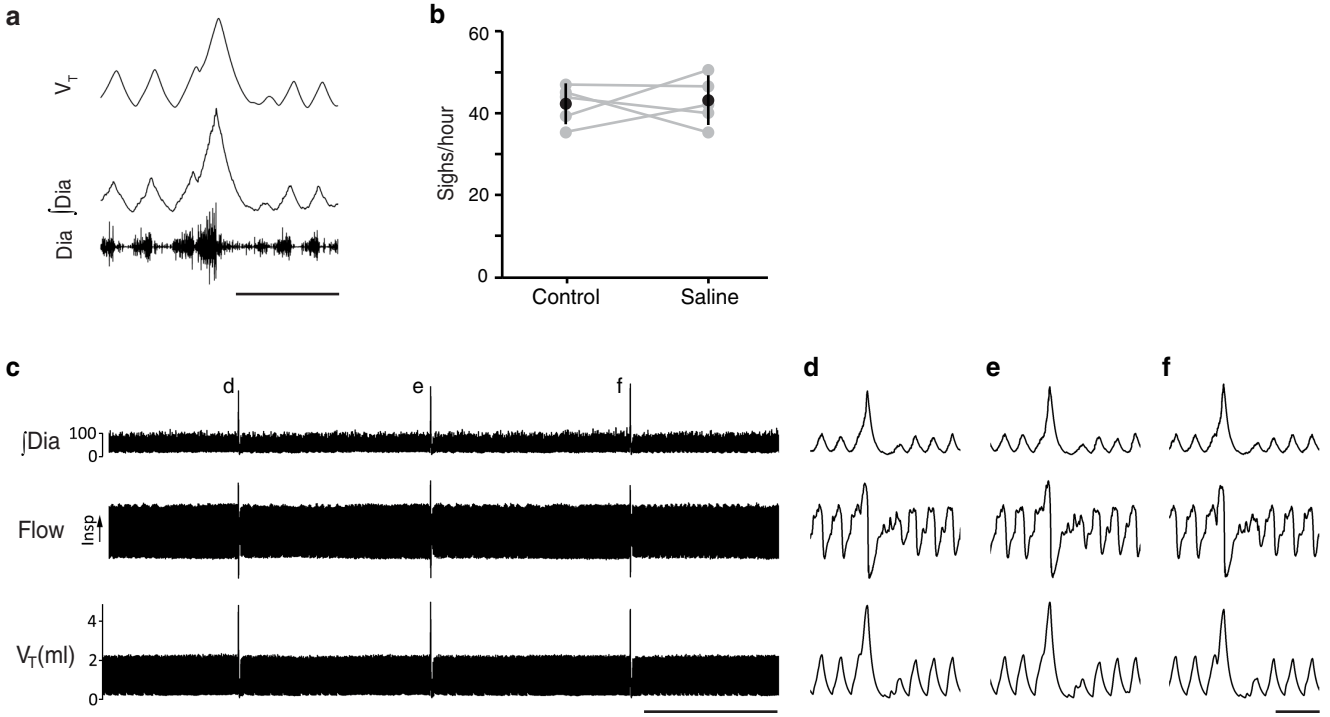

Extended Data Figure 3 | Sighing after surgery and bilateral injection of saline into preBötC. a, Example of a sigh in a breathing activity trace of a urethane anaesthetized rat after surgery as in Fig. 2a–c. V_T, tidal volume; ∫Dia, integrated diaphragm activity; Dia, raw diaphragm activity trace. **b**, Sigh rate before (control) and after (saline) bilateral saline injection into preBötC. There is no effect of saline injection (data are mean ± s.d., $n = 5$, $P = 0.83$ by paired t-test). **c–f**, Breathing activity trace as in **a** (but also showing airflow). Note stereotyped waveform of sighs (**d–f**). Bars, 1 min (**c**), 1 s (**d–f**).

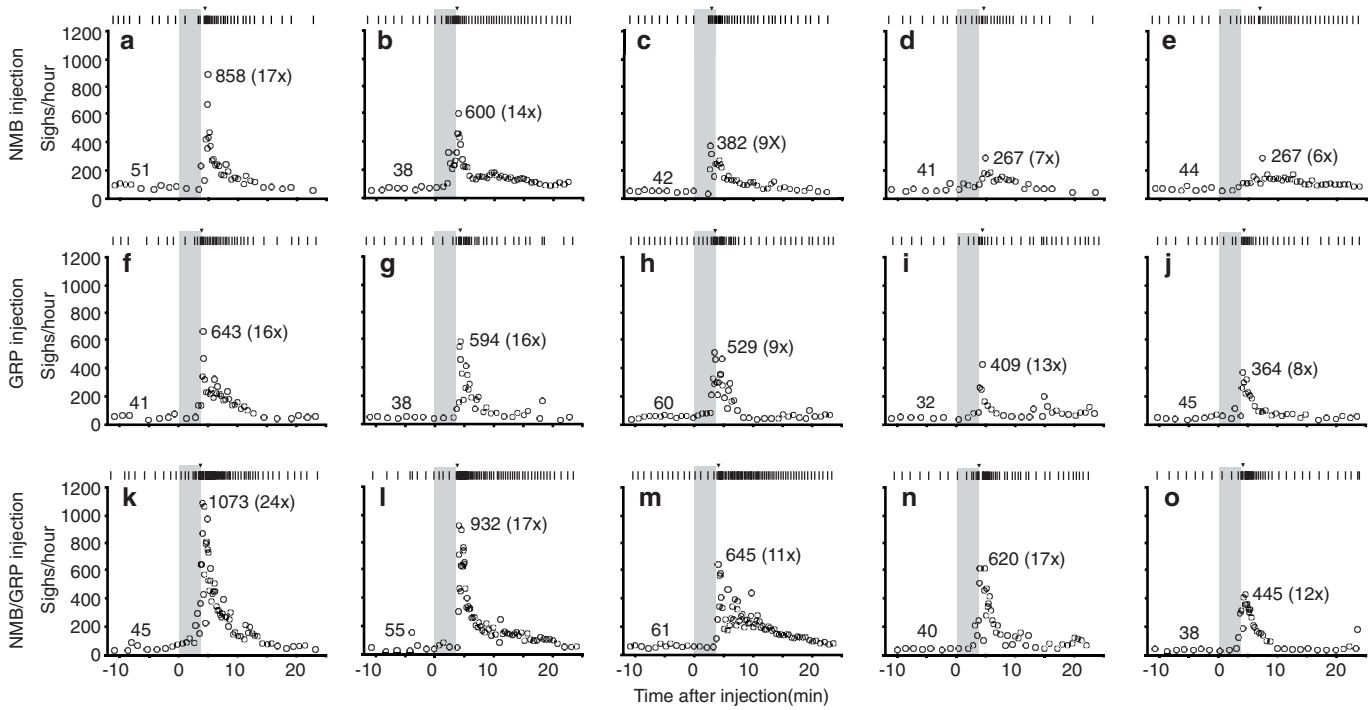

Extended Data Figure 4 | Effects on sighing in individual rats following bilateral injection into preBötC of NMB, GRP and both NMB/GRP. **a**–**e**, Raster plot of sighs (upper) and instantaneous sigh rates (lower) before and after NMB injection for the five experiments (**a**–**e**) shown in Fig. 2d. **f**–**j**, Raster plot of sighs (upper) and instantaneous sigh rates (lower) before and after GRP injection for the five experiments (**f**–**j**) shown in Fig. 3c. **k**–**o**, Raster plot of sighs (upper) and instantaneous sigh rates (lower) before and after NMB/GRP injection for the five experiments (**k**–**o**) shown in Fig. 4i. Grey, injection period; arrowhead in raster plots, maximum instantaneous sigh rate; numbers, basal (left) and maximal instantaneous sigh rate (right) and fold induction (in parentheses) after neuropeptide injection.

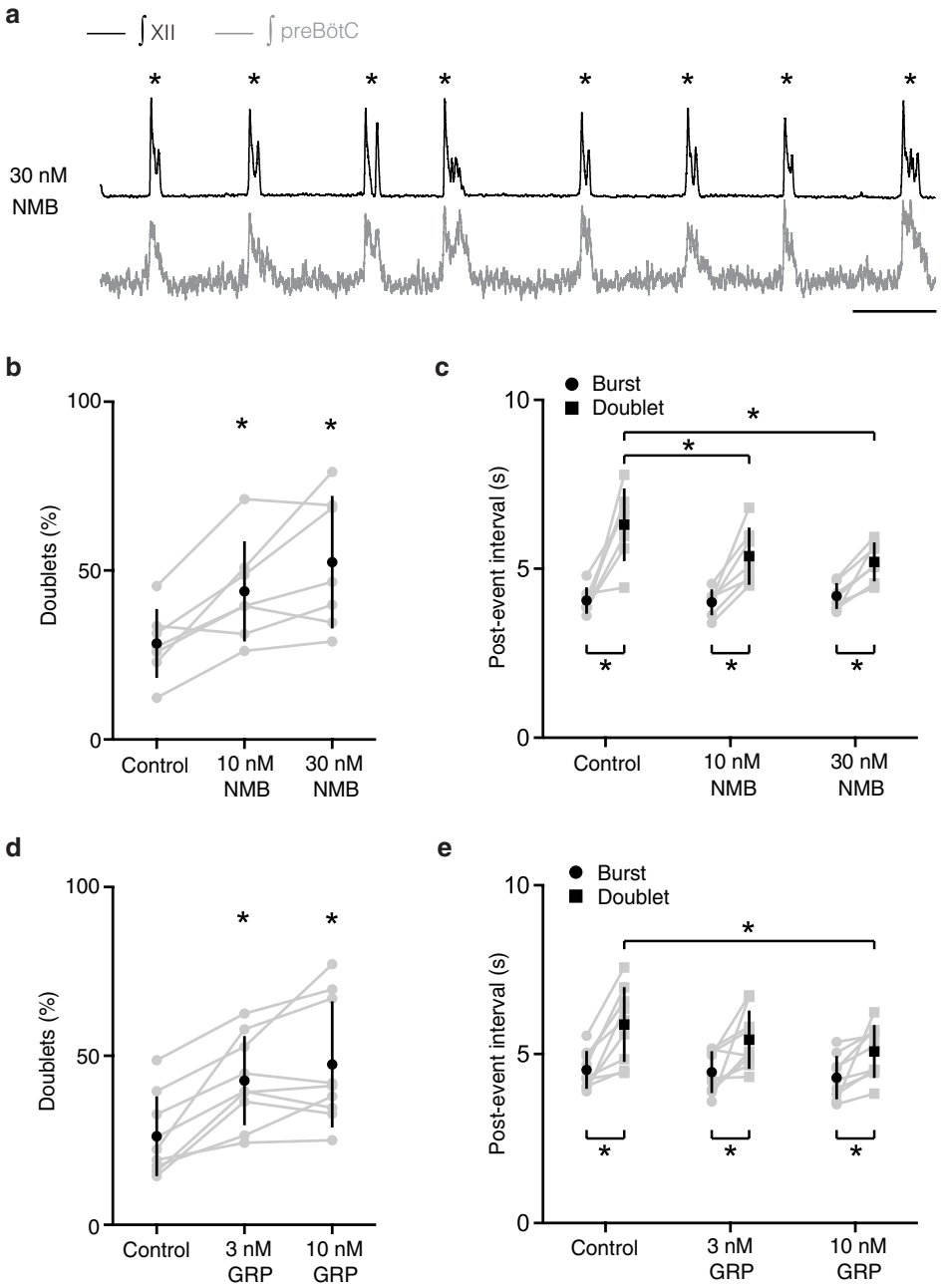

Extended Data Figure 5 | Effect of NMB and GRP on rhythmic activity of preBötC slice. a, Neuronal activity trace(∫XII, black; ∫preBötC population activity, grey) of preBötC slice containing 30 nM NMB, as in Fig. 2e. Note the extreme effect of NMB in which every burst ('breath') in the trace is a doublet ('sigh', asterisk). Bar, 5 s. **b**, **c**, NMB increases the doublet rate by increasing the fraction of total events that are doublets (**b**) and decreasing the interval following a doublet (**c**). Data are mean ± s.d., $*P < 0.05$ by paired *t*-test, $n = 7$. **d**, **e**, GRP also increases the doublet rate by increasing the fraction of total events that are doublets (**d**) and decreasing the interval following a doublet (**e**). Data are mean ± s.d., $*P < 0.05$ by paired *t*-test, $n = 9$. Note that post-doublet intervals are significantly longer than post-burst intervals under all conditions, consistent with longer post-sigh apneas *in vivo*.

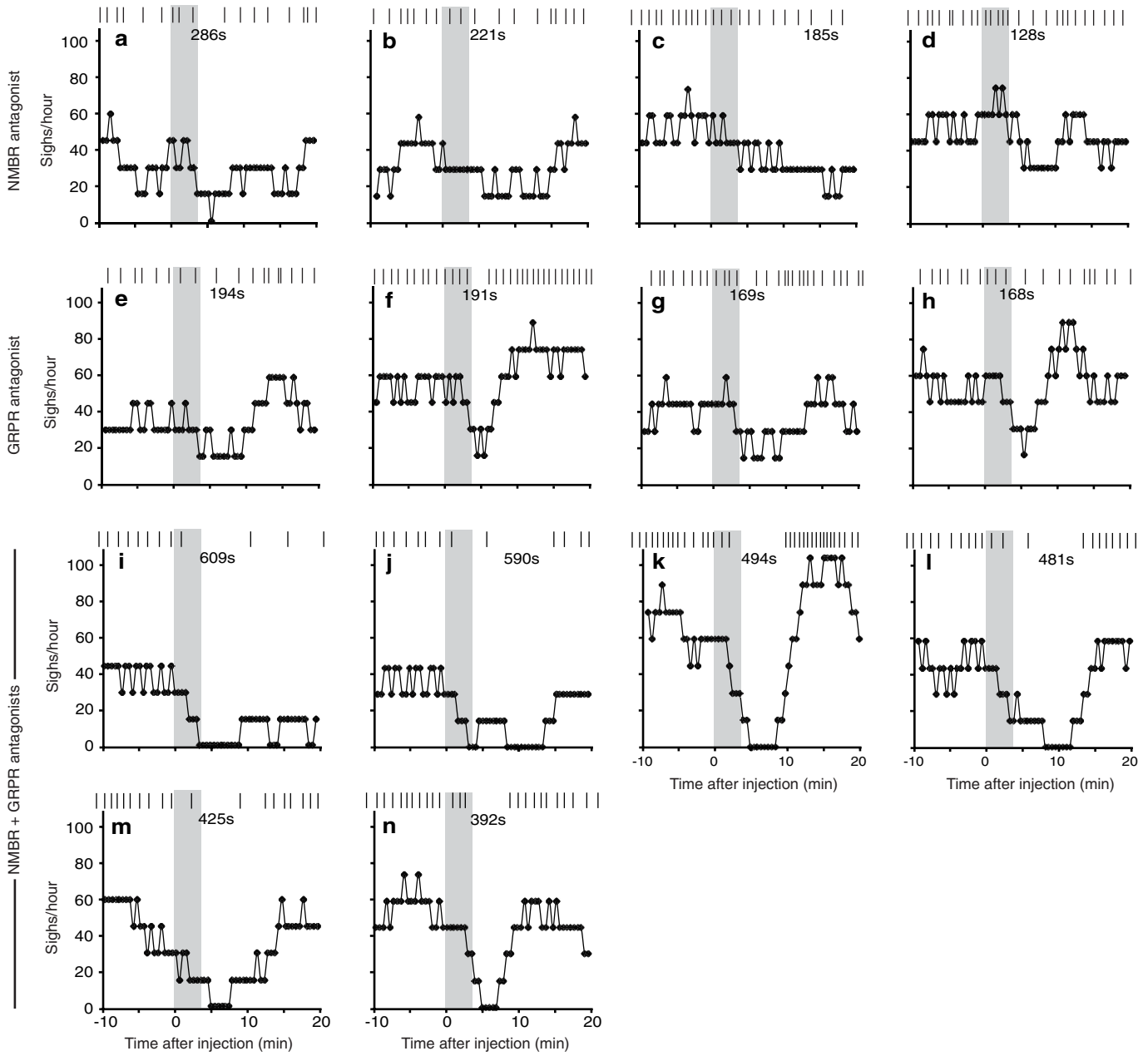

Extended Data Figure 6 | Effects on sighing in individual rats following bilateral injection of BIM23042, RC3095 and BIM23042/RC3095 into preBötC. a–d, Raster plot of sighs (upper) and binned sigh rates (lower; bin size 4 min; slide 30 s) before and after injection of the NMBR antagonist BIM23042 for the four experiments shown in Fig. 2h. **e–h**, Raster plot of sighs (upper) and binned sigh rates (lower; bin size 4 min; slide 30 s) before and after injection of the GRPR antagonist RC3095 for the four experiments shown in Fig. 3f. **i–n**, Raster plot of sighs (upper) and binned sigh rates (lower; bin size 4 min; slide 30 s) before and after BIM23042 and RC3095 injection for the six experiments shown in Fig. 4j. Grey, injection period; numbers, longest inter-sigh intervals (s, seconds) following injection.

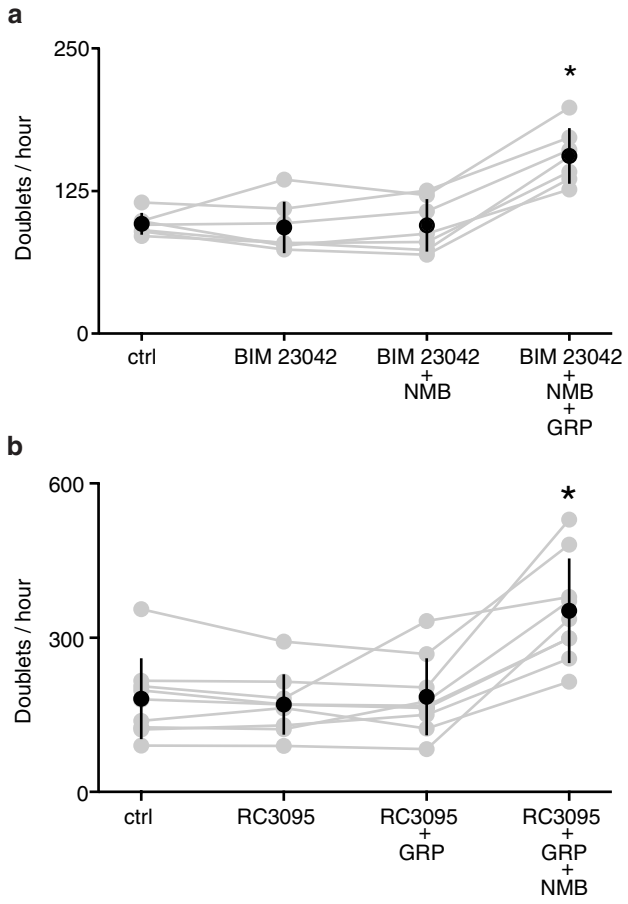

Extended Data Figure 7 | Specificity of antagonists BIM23042 and RC3095 in preBötC slice. a, BIM 23042 (100 nM) blocks the effect of NMB (10 nM), but not GRP (3 nM) in preBötC slices. Data are mean ± s.d., $*P < 0.05$ by paired *t*-test, $n = 7$. **b**, RC3095 (100 nM) shows the opposite specificity, blocking the effect of GRP (3 nM), but not NMB (10 nM). Data are mean ± s.d., $*P < 0.05$ by paired *t*-test, $n = 9$.

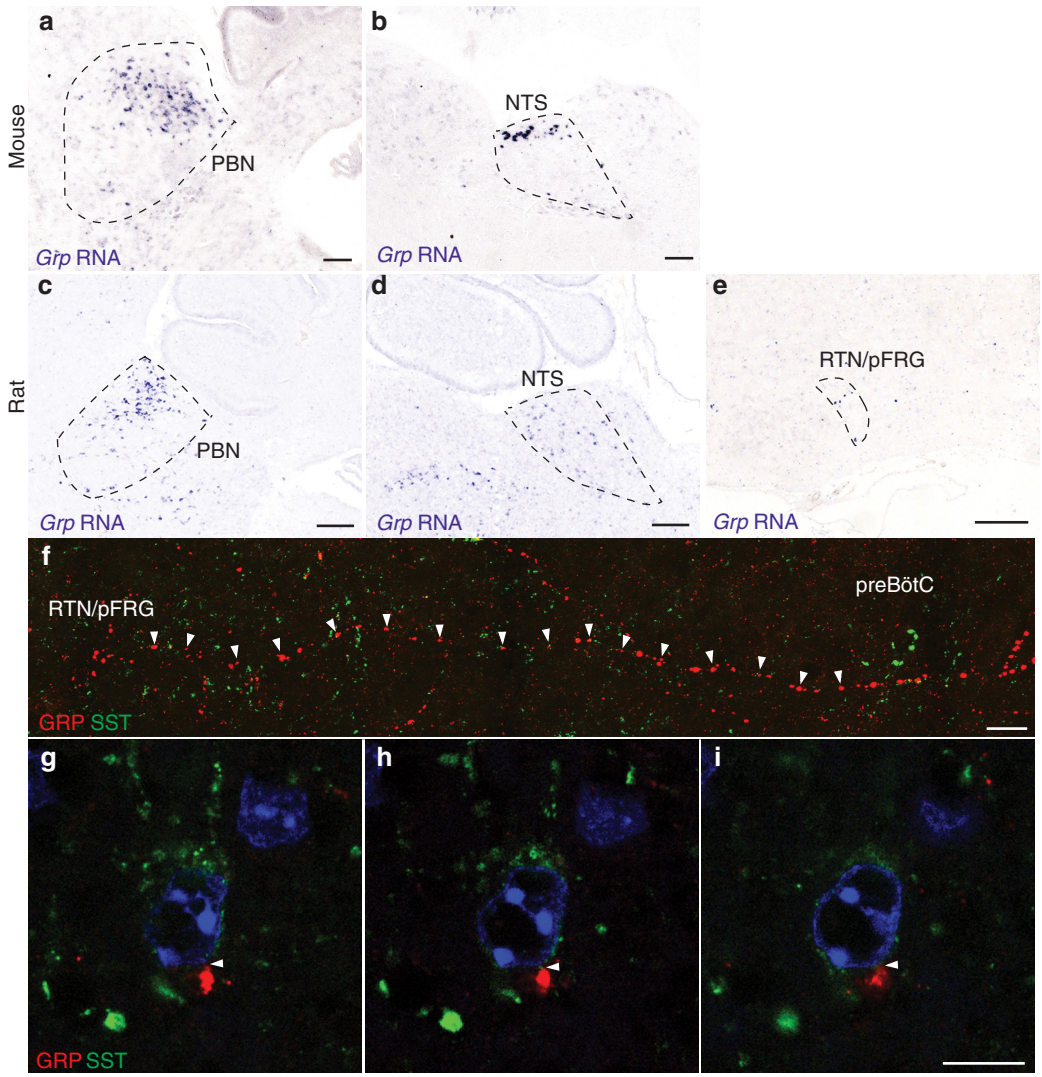

Extended Data Figure 8 | Expression of *Grp* in rodent brain. a, **b**, *In situ* hybridization of mouse brain slices as in Fig. 3a showing expression of *Grp* (purple) in parabrachial nucleus (PBN) (**a**) and nucleus tractus solitarius (NTS) (**b**). Scale bar, 200 μm. **c**–**e**, *In situ* hybridization of rat brain slices showing expression of *Grp* in PBN (**c**), NTS (**d**), RTN/pFRG (**e**). Scale bar, 200 μm. **f**, Tiled image showing GRP-positive projection (red) from RTN/pFRG region to preBötC region containing SST-positive neuron (green). Scale bar, 20 μm. **g**–**i**, Serial confocal optical sections (0.8 μm apart) through mouse preBötC stained for GRP (red) and SST (green) focusing on short segment of GRP-positive projection where a GRP puncta (red) directly abuts (arrowhead) an SST-positive neuron. Scale bar, 10 μm.

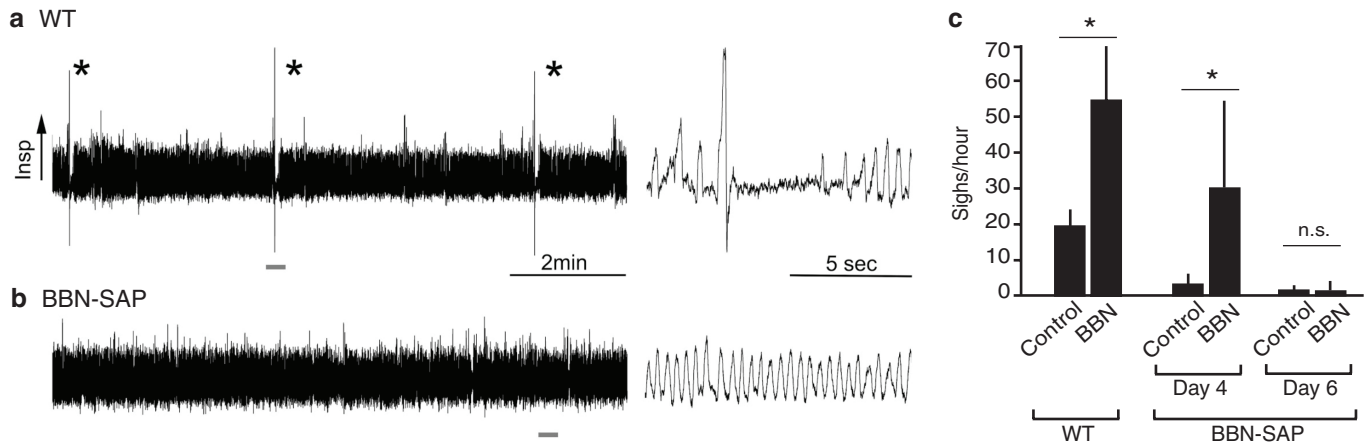

Extended Data Figure 9 | Effect of bombesin injection on sighing following BBN–SAP-induced ablation of NMBR-expressing and GRPR-expressing preBötC neurons. a, **b**, 10 min plethysmography traces of a control rat (**a**) and a day 5 BBN–SAP injected rat (**b**) during eupneic breathing (left). Indicated parts (10 s) of traces are expanded at right. Note presence of sighs with stereotyped waveform in control rat, and no sighs detectable in BBN–SAP injected rat. **c**, Sigh rate before (control) and after 10 μg bombesin injection (BBN) into the cisterna magna of rats before BBN–SAP injection (WT) and at day 4 and day 6 after BBN–SAP injection (BBN–SAP) into the preBötC to ablate NMBR-expressing and GRPR-expressing neurons as in Fig. 5a, b. Values shown are mean ± s.d. (WT, $n = 10$; BBN–SAP, $n = 7$ for day 4 and $n = 5$ for day 6), $^*P < 0.05$ by paired t-test; n.s., not significant.